

# Photon-stimulated ion desorption from molybdenum oxides following Mo $2p_{3/2}$ excitation

Guohua Wu<sup>a,b\*</sup>, Yuji Baba<sup>a</sup>, Tetsuhiro Sekiguchi<sup>a</sup> and Iwao Shimoyama<sup>a</sup>

<sup>a</sup>Synchrotron Radiation Research Center, Japan Atomic Energy Research Institute, Tokai-mura, Naka-gun, Ibaraki-ken, 319-1195, Japan

<sup>b</sup>National Synchrotron Radiation Laboratory, University of Science and Technology of China, Hefei, Anhui, 230026, China. E-mail: [ghwu@ustc.edu.cn](mailto:ghwu@ustc.edu.cn)

Photon-stimulated ion desorption from solid MoO<sub>3</sub> following the Mo  $2p_{3/2}$  resonant transition has been investigated. In the XANES spectrum, Mo  $2p_{3/2}$  peak is split into two components corresponding to the excitations from Mo  $2p_{3/2}$  into the  $t_{2g}$  and  $e_g$  orbitals. It was observed that the desorption yield of O<sup>+</sup> ions at the Mo  $2p_{3/2} \rightarrow e_g$  resonance is higher than that at the Mo  $2p_{3/2} \rightarrow t_{2g}$  resonance. The Auger decay spectra reveal that there exist two kinds of spectator Auger decays. The high desorption yield at the  $2p_{3/2} \rightarrow e_g$  resonance is interpreted by the fast breaking of the Mo-O bond due to the localization of the electrons in the highly antibonding  $e_g$ .

**Keywords:** photon-stimulated ion desorption, XANES, molybdenum oxides, Mo  $2p_{3/2}$  excitation.

## 1. Introduction

It is well known that irradiation of x-rays on solid surface can induce various chemical changes such as decomposition and desorption. The inner-shell electron excitation by x-ray irradiation is primarily localized around the specific element or chemical bond being excited, owing to the localized nature of the inner-shell electrons. Some examples for specific chemical bond scission and ion desorption induced by core-level excitation have been reported for adsorbed molecules on solid surfaces (Baba *et al.*, 1997). For bulk material, such a specific chemical reaction by core-level excitation has been scarcely reported, because the secondary electrons produced after Auger decay also induce non-specific reaction.

In the present paper, photon-stimulated ion desorption (PSID) from bulk oxide following the specific inner-shell electron excitation is investigated using monochromatized synchrotron radiation. Here, we have chosen MoO<sub>3</sub> as a sample, because this material is of great importance in catalysis, and also this material is known to be highly volatile and its surface is sensitive to irradiation of UV light, X-rays, electrons and ions (Werfel *et al.*, 1983). The mechanism of the decomposition and ion desorption is discussed on the basis of the photon-energy dependencies of the ion yields and electron yields around the photon-energy of the Mo  $2p_{3/2}$  threshold. For clarifying the electron relaxation processes following the inner-shell electron excitation, the Auger decay spectra after the excitation around the Mo  $2p_{3/2}$  threshold are also presented.

## 2. Experimental

The experiments were carried out at the BL-27A station of the Photon Factory in High Energy Accelerator Research Organization. A double-crystal of the InSb(111) plane was used as a monochromator. The energy resolution was 1.2 eV at Mo  $2p_{3/2}$  edge.

The apparatus has been described in detail elsewhere (Baba *et al.*, 1995). Briefly, the ultra-high vacuum system (base pressure around  $1 \times 10^{-8}$  Pa) consisted of a quadrupole mass spectrometer

(ULVAC MSQ-1000), a hemispherical electron energy analyzer (VSW CLASS-100) and a sputter ion gun. MoO<sub>3</sub> sample was prepared by oxidizing polycrystalline Mo foils at 700°C in atmosphere in furnace.

The XANES spectrum was recorded in total electron yield mode (TEY) by measuring the sample drain current. The spectrum was normalized by the photo-yield of a clean copper mesh located in front of the sample. The desorbed ions were detected by a quadrupole mass spectrometer operating in a pulse-counting mode. The sample was biased at +40 V during the PSID measurements.

Sample charging effects have been ruled out during the measurements of the Auger electron spectra by applying an electron flood gun with constant electron energy.

## 3. Results and discussion

### 3.1. XANES spectrum

XANES spectrum of solid MoO<sub>3</sub> in the vicinity of the molybdenum  $2p_{3/2}$  edge is presented in Fig. 1(A, bottom). As shown, the prominent feature in this spectrum is a doublet structure labeled 1 and 2 with energies at 2523.9 and 2526.6 eV respectively. The similar structure was also observed by Evans *et al.* (1991) in the smoothed second derivative of the Mo L<sub>III</sub> edge for MoO<sub>3</sub>, and by Bare *et al.* (1993) in the Mo L<sub>III</sub> edge XANES spectrum of dispersed MoO<sub>3</sub> catalysis taken in fluorescence yield mode. In solid MoO<sub>3</sub>, Mo atom is surrounded by an octahedron of O ligands. According to a ligand-field approach, the molybdenum 4d orbitals split into  $t_{2g}$  and  $e_g$  orbitals by the octahedral ligand-field of oxygen. So the doublet structure in the XANES spectrum is attributed to the resonant transitions from the Mo  $2p_{3/2}$  ground state to the lowest unoccupied antibonding orbitals  $t_{2g}(d\pi^*)$  and  $e_g(d\sigma^*)$  respectively. It is known that the  $e_g$  orbitals have higher energy than  $t_{2g}$  under octahedral field. Thus the feature at 2523.9 eV comes from the transition to the  $t_{2g}$  orbital, whereas the one at 2526.6 eV comes from the transition to  $e_g$  orbital.

### 3.2. Photon-energy dependence of ion desorption

According to the mass spectrum of ions desorbed from the solid MoO<sub>3</sub>, the dominant ions desorbed from the sample surface were O<sup>+</sup> ions. The photon-energy dependence of the O<sup>+</sup> yield is shown in Fig. 1(B, top). It is observed that the desorption yield around the peak 2 (2526.6 eV) is higher than that at peak 1, which is evidently reverse to the total electron yield.

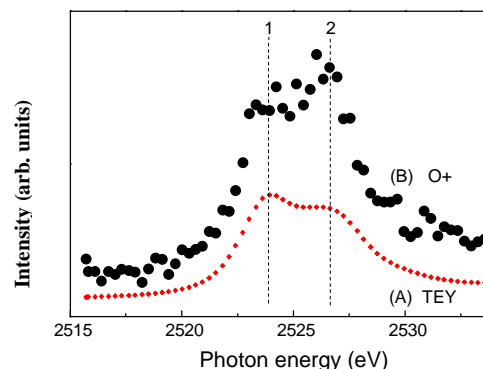


**Figure 1**

Photon-energy dependence at Mo  $2p_{3/2}$  edge of: (A) total electron yield, and (B) desorption yield of O<sup>+</sup> ions.

### 3.3. Auger decay

In order to understand the mechanism of ion desorption, it is essential to investigate the total de-excitation processes following

the resonant core-level excitation. For low-Z elements, a resonant Auger decay is the main primary de-excitation process other than x-ray fluorescence. As for  $\text{MoO}_3$ , since the x-ray fluorescence yield is less than 5% of the total de-excitation processes (Krause, 1979), the dominant primary de-excitation channel following the Mo  $2p_{3/2}$  excitation should be a resonant Auger decay. The electronic decay processes of molecules following the resonant photo-excitation from core level to valence unoccupied orbital can happen via two principal Auger decay ways (Carson et al., 1988), i.e., the spectator Auger and the participator Auger transitions. These two kinds of Auger processes can be distinguished by the different kinetic energy in the Auger electron spectra. The participator Auger process results in a final electronic configuration of a one-hole state, which is similar to the direct photoemission process. Therefore, if the participator Auger is significant, the relative intensity of the corresponding photoelectron peak will be changed dramatically as compared with those in the normal photoemission spectra (Chen, et al. 1996). However, the intensities of any photoelectron peaks were scarcely changed following the Mo  $2p_{3/2}$  excitation, therefore this process is negligible in the present case. In contrast, the spectator Auger transition should appear around the corresponding normal Auger position but there exists slightly shifted kinetic energies.

The resonant Auger decay spectra around the Mo  $L_3M_{4,5}M_{4,5}$  region at various photon energies are shown in Fig. 2. The number indicated in each spectrum corresponds to the photon energy used for the excitation. It is obvious that the Mo  $L_3M_{4,5}M_{4,5}$  spectator Auger process is the predominant decay channel at resonance region. A three-peak feature (labeled with A, B and C) appeared from the spectrum of 2520.9 eV excitation. The intensity of this feature increased with the photon energy and reached its maximum around 2523.9 eV. These peaks have been assigned as the spectator Auger transitions (Sasaki, et al. 1994).

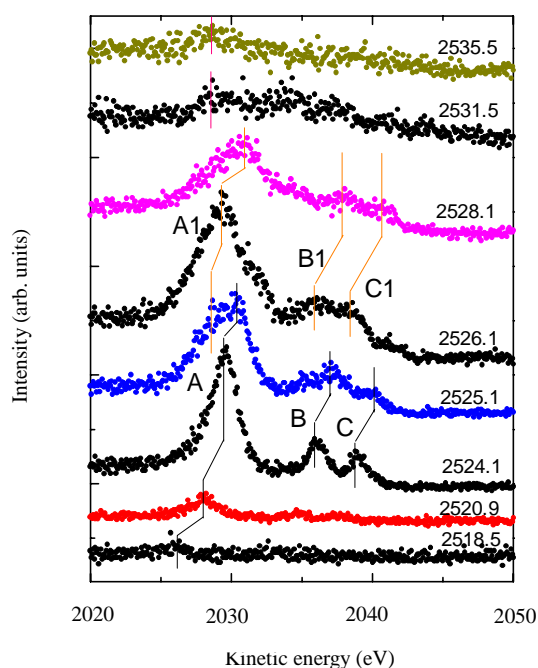


**Figure 2**

Auger decay spectra for  $\text{MoO}_3$  excited by various photon energies around the Mo  $2p_{3/2}$  edge.

The linear kinetic energy dispersion with the incident photon energy was considered to be a result of the bandlike structure of the unoccupied orbitals in solids and the Auger resonance Raman

process. However, a remarkable difference observed in the present Auger electron spectra is that, there exists another three-peak feature (labeled with A<sub>1</sub>, B<sub>1</sub> and C<sub>1</sub>) appeared from the spectrum of 2525.1 eV (the first three-peak structure still exists at this energy). Its intensity also increased with the photon energy, and reached its climax near 2526.1 eV. A similar kinetic energy shift toward higher energy can be observed. This finding suggests that there exist two kinds of spectator Auger decays in this energy region. We call the first one (appearing at lower energy) as spectator I and the other as spectator II. The normal Auger line apparently begins to appear from the spectrum around 2528.1 eV, and its kinetic energy is almost constant. Comparing these Auger decay spectra with the XANES (Fig. 1A), it is easy to find that the spectator I process is responsible for the peak 1 of the XANES and the spectator II process is mainly for the peak 2.

### 3.4. Mechanism of ion desorption

It is extensively accepted that the ion desorption following core-level excitation can be mostly interpreted in terms of the KF model, namely Auger-initiated desorption (Knotek et al. 1978). This is reliable especially for most multilayered adsorbate and bulk materials. In this model, the Auger decay following core excitation leads to a multi-hole final state. Then ion desorption occurs as a result of the Coulomb repulsion of the highly charged species on the surface. In this case, the photon-energy dependence of the ion yield would be roughly similar to the x-ray absorption spectrum. Since there exists obvious dissimilarity between the TEY spectrum and the O<sup>+</sup> PSID spectrum, it is suggested that there exist other processes for O<sup>+</sup> desorption. The significance of the spectator electron on ionic desorption has been proposed by Ramarker (1983) and demonstrated by other authors (Baba et al. 1996). Generally, the 2-holes and 1-electron final state following the resonant core-level excitation is more effective for ion desorption than the 2-hole state originating from the normal Auger decay. On the basis of the analysis of Auger electron spectra, the transitions from the Mo  $2p_{3/2}$  to  $t_{2g}$  and  $e_g$  are primarily followed by the spectator I and II Auger decay processes, respectively. The important point is that the excited electrons in the  $t_{2g}$  and  $e_g$  orbitals remain in these states during the Auger decay, and these electrons are localized in the respective orbitals.

It is known that the  $t_{2g}$  state is mainly composed of  $d_{xy}$ ,  $d_{yz}$  and  $d_{zx}$  orbitals and it has  $\pi^*$ -like character. While the  $e_g$  state is composed of  $d_{z^2}$  and  $d_{x^2-y^2}$  orbitals with  $\sigma^*$ -like character. It is considered that the existence of electron in the antibonding  $\sigma^*$  state would induce highly repulsive state compared with that in the  $\pi^*$  state. We consider that such highly repulsive state after Mo  $2p_{3/2} \rightarrow e_g$  excitation results in the fast bond breaking so that the ions leave the surface quickly enough before neutralization. We consider that this is the reason why the desorption yield at the Mo  $2p_{3/2} \rightarrow e_g$  resonance is higher than that at the Mo  $2p_{3/2} \rightarrow t_{2g}$  one which is reverse to the electron yield. The measurements on the PSID and Auger decay spectra at the other absorption edges are now in progress to elucidate this speculation more clearly.

For multilayered adsorbate and bulk materials, it has been generally accepted that ion desorption by core excitation does not necessarily originate from the localized excitation on or near the desorbing atom but rather from a delocalized excitation with a long-range indirect processes such as secondary-electron-induced process. However, our results show that even for bulk material like  $\text{MoO}_3$ , the chemical bond breaking is induced not only by the secondary electron effect, but also by the specific direct core-to-valence excitation process. This result will shed light on the site-selective fragmentation in the other bulk materials.

#### 4. Conclusions

The Mo  $2p_{3/2}$  resonant transition is split into two components, which correspond to the excitations from the Mo  $2p_{3/2}$  to the  $t_{2g}$  and  $e_g$  antibonding orbitals. The Auger decay spectra reveal that these transitions are mostly followed by the molybdenum  $L_3M_{4,5}M_{4,5}$  spectator Auger decay. The spectra also demonstrate that there exist two kinds of spectator Auger decays around the Mo  $2p_{3/2}$  edge, corresponding the transitions from the Mo  $2p_{3/2}$  to the  $e_g$  and  $t_{2g}$  states, respectively. The spectator Auger processes and localization of the spectator electrons in the respective antibonding orbitals is the main trigger of the desorption of  $O^+$  ions. The high desorption yields at the Mo  $2p_{3/2} \rightarrow e_g$  resonance is interpreted by the localization of the electrons in the  $\sigma^*$ -like antibonding state which results in the fast bond breaking.

The authors would like to thank the staff of Photon Factory of the High Energy Accelerator Research Organization (KEK-PF) for their assistance throughout the experiments.

#### References

- Baba, Y., Yoshii, K. & Sasaki, T. A. (1995). *Surf. Sci.* **341**, 190-195.  
Baba, Y., Yoshii, K. & Sasaki, T. A. (1996). *J. Chem. Phys.* **105**, 8858-8864.  
Baba, Y., Yoshii, K. & Sasaki, T. A. (1997). *Surf. Sci.* **376**, 330-338.  
Bare, S. R., Michell, G. E., Maj, J. J., Vrieland, G. E. & Gland, J. L. (1993). *J. Phys. Chem.*, **97**, 6048-6053.  
Carlson, T. A., Gerard, P., Krause, M. O., von Wald, G., Taylor, J. W., Grimm, F. A. & Pullen, B. P. (1988) *J. Electron Spectrosc. Relat. Phenom.* **47**, 227-243.  
Chen, J. M., Klauser, R., Cheng, S. I., Yang, S. C., Hsu, Y. J., Wen, C. R. (1996). *Phys. Rev. B*, **54**, 1455-1458.  
Evans, J. & Mosselmans, J. F. W. (1991). *J. Phys. Chem.*, **95**, 9673-9676.  
Grunes, L. A. (1983). *Phys. Rev. B*, **27**, 2111-2131.  
Krause, M. O. (1979). *J. Phys. Chem. Ref. Data*, **8**, 307-328.  
Knotek, M. L. & Feibelman, P. J. (1978). *Phys. Rev. Lett.* **40**, 964-967.  
Ramarker, D. E. (1983). *Chem. Phys.* **80**, 183-202.  
Sasaki, T. A., Baba, Y., Yoshii, K. & Yamamoto, H. (1994). *Phys. Rev. B* **50**, 15519-15526.  
Werfel, F. & Minni, E. (1983). *J. Phys. C: Solid State Phys.*, **16**, 6091-6100.